Angewandte Chemie
Eine Zeitschrift der Gesellschaft Deutscher Chemiker

Supporting Information

Precisely Tailoring Upconversion Dynamics via Energy Migration in Core–Shell Nanostructures

Jing Zuo[+], Dapeng Sun[+], Langping Tu[+], Yanni Wu, Yinghui Cao, Bin Xue, Youlin Zhang, Yulei Chang, Xiaomin Liu, Xianggui Kong, Wybren Jan Buma, Evert Jan Meijer,* and Hong Zhang**

anie_201711606_sm_miscellaneous_information.pdf

Supporting Information

Experimental section

Reagents. $LnCl_3 \cdot 6H_2O$ (Ln: Y, Yb, Er >99%), Ln_2O_3 (Ln: Y, Yb, Er, Nd >99%), Oleic acid (OA, 90%), 1-Octadecene (ODE, 90%), Oleylamine (OM, 90%), sodium trifluoroacetate (98%) and trifluoroacetic acid (99%) were purchased from Sigma-Aldrich and used without further purification. NaOH (>98%), NH_4F (>98%), methanol, ethanol and cyclohexane were purchased from GFS Chemical.

Synthesis of 20 nm *β*-$NaYF_4$: 20% Yb, 2% Er bare core nanoparticles. The 20 nm β-$NaYF_4$:Yb,Er nanoparticles were synthesized following reported approach.[1] Typically, 0.78 mmol $YCl_3 \cdot 6H_2O$, 0.2 mmol $YbCl_3 \cdot 6H_2O$, 0.02 mmol $ErCl_3 \cdot 6H_2O$ were added into a mixture of 6 mL OA, 15 mL ODE in a three-necked flask. The solution was heated to 160 ℃ for 20 min under argon atmosphere to form a transparent solution and then cooled down to room temperature. Subsequently, 10 mL methanol solution contains 100 mg NaOH and 148 mg NH_4F was added into the solution dropwise. The mixed solution was heated slowly to 70℃ and kept stirring for 30 minutes to remove the methanol solvent completely. After the evaporation of methanol, the solution was heated to 300℃ and maintained for 1.5 hours under argon atmosphere. After cooled down to room temperature, the resultant mixture was washed with ethanol and purified by centrifuge 3 times at the speed of 7000 rpm (each time for 6 minutes). The as-synthesized product of 20 nm *β*-$NaYF_4$: 20% Yb, 2% Er core nanoparticles were dispersed in 4 mL cyclohexane.

Synthesis of the *β*-core/shell nanoparticles. The $NaYF_4$: 20% Yb, 2% Er@$NaYF_4$ (YbEr@Y), $NaYF_4$: 20% Yb, 2% Er@$NaYF_4$: 20% Yb (YbEr@Yb) nanoparticles were synthesized following a reported approach.[1] Take the structure of 1:1 (core: shell) in mol ratio as an example, 1 mmol $LnCl_3 \cdot 6H_2O$ was added into the mixture of 6 ml OA and 15 ml ODE in a three-neck flask. The solution was heated to 160℃ for 20 minutes under argon atmosphere to form a transparent solution and then cooled down to room temperature. Subsequently, 10 mL methanol solution containing 100 mg NaOH and 148 mg NH_4F was added into the solution dropwise. The mixed solution was heated slowly to 70℃ and kept stirring for 30 minutes to remove the methanol solvent completely. After the evaporation of methanol, the cyclohexane solution containing 1 mmol bare core nanoparticles was added into the stirring solution. Then the mixture was heated slowly to 85℃ and kept stirring for another 30 minutes to remove the cyclohexane solvent completely. After the evaporation of cyclohexane, the solution was heated up to 300℃ and maintained for 1h under argon

atmosphere. After cooled down to room temperature, the resultant mixture was washed with ethanol and purified by centrifuge 3 times at the speed of 7000 rpm (each time for 6 minutes). The obtained core-shell nanoparticles (1:1, mol ratio) were dispersed in 8 ml cyclohexane. The shell thickness is controlled by the added mol amount of the shell reactant.

Synthesis of the shell precursors. The cubic sacrificial nanocrystals of 1) $NaYF_4$: 20% Yb, 2) $NaLuF_4$: x%Yb (x=10, 20, 40), 3) $NaYF_4$: 20%Yb, 10% Nd and 4) $NaYF_4$: 20% Nd were synthesized respectively as shell precursors following the reported method.[2] Take 1mmol $NaYF_4$ shell precursor as an example. Add 1 mmol CF_3COONa and 1 mmol $(CF_3COO)_3Y$ into a three-necked flask with 3 ml OA, 3ml OM and 5ml ODE. The solution was heated to 120℃with robust stirring under argon atmosphere for 30 minutes. After the solid reagents were dissolved, the as-obtained clear solution was heated to 290℃ and kept reacting for 45 minutes under argon atmosphere. Then the solution was cooled down to room temperature and washed by ethanol once with centrifuge of 7000 rpm for 6 minutes. The product is dispersed in 4 ml ODE for later use.

Synthesis of the *β*-core/shell/shell nanoparticles. The $NaYF_4$: 20% Yb, 2% Er@$NaYF_4$: 20%Yb@$NaYF_4$: 20%Yb, 10% Nd (YbEr@Yb@YbNd) and $NaYF_4$: 20% Yb, 2% Er@$NaLuF_4$: x%Yb (x=10/20/40) @$NaYF_4$: 20% Nd (YbEr@Yb@Nd) core/shell/shell nanoparticles were prepared following the reported approach.[2] After the reaction for bare core structure, instead of being cooled down, the as-obtained solution was kept at 300℃. Then the cubic sacrificial nanocrystals prepared as shell precursor was injected into the bare core reaction solution in one-shot within ~1 sec by a syringe with a stainless steel cannula. The mixture was ripened with stirring at 300℃ under argon atmosphere to form the core/shell structure. The multi-layer shells were realized by multi-injections. For each injection, the ripening time was 30 minutes for one layer. The shell thickness of each layer is controlled by the amount of cubic sacrificial nanocrystals in each injection. After the ripening, the solution was cooled down to room temperature and washed by ethanol with centrifuge at 7000 rpm 3 times, each for 6 minutes. The as-obtained nanoparticles were dispersed in 4 mL cyclohexane. The total shell thicknesses were controlled by the total amount of shell precursors.

Characterization. The transmission electron microscopy (TEM) was performed on a Tecnai G2 F20 S-TWIN D573 electron microscope operated at 300 kV TEM. The scanning electron microscopy (SEM) was performed on a Hitachi, S-4800. Power X-ray diffraction (XRD) characterization was performed on a X-ray powder diffractometer with Cu Kα radiation (λ = 1.542Å). The upconversion steady-state emission spectra were collected at room temperature by a Maya 2000 visible spectrometer (Ocean optics). All the luminescence dynamics were recorded with a 500 MHz Tektronix digital oscilloscope and the excitation was realized by a nanosecond pulse train at 800 nm or 980 nm from an optical parametric oscillator.

During the spectroscopic measurements all the samples were dispersed in cyclohexane with the same concentration of nanoparticles.

Binary pulse excitation scheme. The setup consists of two Q-swiched Nd-YAG optical parametric oscillator lasers (8 ns, 10 Hz, 1mJ). The wavelengths of laser pulses are set at 800 nm and 980 nm, respectively. The time gap between two pulses is adjusted by a digital delay generator (Model 588 - 1U Rack Mount 8 Channel DDG). The $NaYF_4$: 20% Yb, 2% Er @$NaYF_4$: 20% Yb @$NaYF_4$: 10% Nd, 20%Yb (YbEr@Yb@YbNd) upconversion nanoparticles were dispersed in cyclohexane with the concentration of 10 mg/ml.

Simulation section

1: Basic picture of simulation model.

The Monte Carlo simulation model of UC was set up according to a three-dimensional random walk of excited states in the sublattice (consisted by sensitizer and activator ions), and the UC is induced by the "collision" of two or more excited states (Fig. S1). In contrast to previously reported models of UC phenomena related to Monte Carlo simulation or DFT (density functional theory) calculation,[3] our model includes three significant features: 1) It not only simulates the energy migration process, but also contains the light absorption and UC emission processes. Thus it offers a clear microscopic vision of entire UC process from light absorption to UC emission. 2) It is particularly advantageous in dealing with the situation of complicated nanosystems, such as studying the energy migration on the core-shell interface of heterogeneous structures. 3) By taking time evolution process into the system, it not only can be applied for the steady-state simulation, but also enables us to analyze the UC dynamic processes.

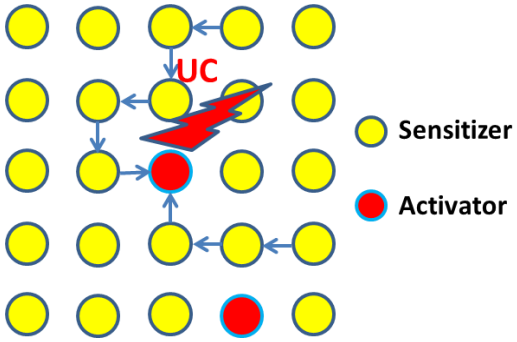

Figure S1. Schematic diagram of the microscopic picture of UC emission which is induced by the "collision" of the randomly walking excited states.

2. Construction of simulation model.

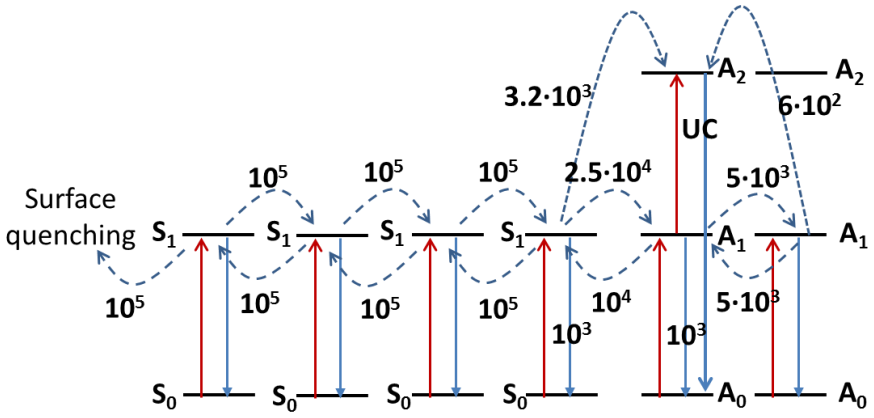

Figure S2. The Monte Carlo simulation model of upconversion processes in the β-$NaYF_4$: 20%Yb, 2% Er nanostructure. $S_{0,1}$ and $A_{0,1,2}$ are the simplified energy levels of sensitizer (Yb^{3+}) and activator (Er^{3+}), respectively. The number labeled in the picture are the interaction rates between energy levels (unit: s^{-1}).

Table S1: The simulation parameters used in this work

Parameters	***Value***
Simulation time period (s)	3
Time step (s)	10^{-6}
Recombination rate of S_1 (s^{-1})*	10^3
Recombination rate of A_1 (s^{-1})*	10^3
Recombination rate of A_2 (s^{-1})*	$7\cdot10^3$
Energy migration rate of $S_1 \rightarrow S_0$ (s^{-1})*	10^5
Energy transfer rate of $S_1 \rightarrow A_0$ (s^{-1})*	$2.5\cdot10^4$
Energy transfer rate of $S_1 \rightarrow A_1$ (s^{-1})*	$3.2\cdot10^3$
Energy transfer rate of $A_1 \rightarrow S_0$ (s^{-1})*	$1.0\cdot10^4$
Energy migration rate of $A_1 \rightarrow A_0$ (s^{-1})*	$5\cdot10^3$
Energy transfer rate of $A_1 \rightarrow A_1$ (s^{-1})*	600
Absorption cross section of S_0 (cm^2)*	$1.17\cdot10^{-20}$
Absorption cross section of A_0 (cm^2)*	$1.7\cdot10^{-21}$
Surface quenching rate (s^{-1})	10^5
Quantum yield of A_2 state	50%

*Calculated from crystal structure of β-$NaYF_4$: 20%Yb, 2% Er (JCPDS: 16-0334).

As a proof of concept simulation, four reasonable simplifications are taken in this work:

1: The construction of nanoparticles: the crystal structure of nanoparticle was simplified to a simple cubic structure which only contains sensitizers and activators. According to the Ln^{3+} doping concertation (*e.g.* 20% sensitizer and 2% activator) and the lattice parameters of hexagonal phase $NaYF_4$ (or $NaLuF_4$) matrix, the calculated distance between the nearest neighboring ions is about 0.8 nm. Therefore, a 20 nm diameter nanoparticle is modeled as a 25×25×25 cube sublattice, which consists 15625 grid points, and each grid point is randomly set as one sensitizer or activator ion with the ratio of 10 to 1.

2: The energy states of ions: as shown in Fig. S2, sensitizer ions have two energy levels (labeled as S_1 and S_0, respectively) and activator ions have three energy levels (labeled as A_2, A_1 and A_0, respectively).

3: The simulation parameters: the advantage of this model is that almost all the simulation parameters can be quantitatively obtained from the experimental results or quantum mechanics calculations. More specifically:

a) the recombination rate of S_1 and $A_{1,2}$ states are obtained from the reciprocal of the measured lifetime of each energy states (*i.e.* ~ 1 ms lifetime for S_1, A_1 states, and ~ 140 μs lifetime for A_2 state).

b) the absorption cross section of S_0 and A_0 are obtained from the previously reports.[4]

c) the quantum yield of A_2 state (*i.e.* 50%) is evaluated from the generally luminescence efficiency of lanthanide ions doped phosphors.

d) based on the assumption that the energy transfer/migration processes only occur between the two closest neighboring ions, their energy transfer/migration probability can be considered as the sum up of three parts:[5]

$$P = \frac{\left(\frac{R_0}{R}\right)^s}{\tau_s} \ (s = 6, 8, 10)$$

1) s=6 for dipole-dipole interactions (P_{dd}),

2) s=8 for dipole-quadrupole interactions (P_{dq}),

3) s=10 for quadrupole-quadrupole interaction(P_{qq}).

Where τ_s is the actual lifetime of the donor excited states, R_0 is the critical transfer distance for which excitation transfer and spontaneous deactivation of the sensitizer have equal probability. R is the real distance between the two ions. From the literature report,[6] if R is fixed to $7a_0$ (a_0=0.53Å), the Yb^{3+}→Yb^{3+} energy migration rate (*i.e.* S_1→S_0) is ~ 1.6×10^8 s^{-1}, more specifically: P_{dd} ~ 2.8×10^6 s^{-1}, P_{dq} ~ 1.4×10^7 s^{-1} and P_{qq} ~ 1.4×10^8 s^{-1}. Accordingly, for the β-$NaYF_4$: 20%Yb, 2% Er nanoparticle where the ion-to-ion distance R' is fixed to ~ 0.8 nm (R' is calculated from the Ln^{3+} ions doping concentration and the lattice parameters of β-$NaYF_4$ or $NaLuF_4$ matrix), three interaction parameters are changed to: P_{dd}' ~ 2.8×10^4 s^{-1}, P_{dq}' ~ 3.0×10^4 s^{-1} and P_{qq}' ~ 6.4×10^4 s^{-1}, and the sum up of three parts is ~ 10^5 s^{-1}, as placed in the Fig. S2 and Table S1.

e) the surface quenching rate is discussed in the following sections (Table S3 and

Fig. S7).

4: Because of the relatively small effects, some secondary processes are reasonably ignored without affecting the basic understanding of the model, including: stimulated emission, cross relaxation ($A_2 + S_0 \rightarrow A_1 + S_1$) and excited states absorption ($A_1 + h\boldsymbol{\upsilon} \rightarrow A_2$) processes, *etc*.

3: Simulation approach

Next, based on the fixed parameters, the UC processes in nanoparticle could be simulated as follows:

(1) For the steady-state UC processes: at the start of the simulation, all the ions were numbered and placed in their ground states. The macroscopic UC phenomena were rebuilt by the statistics of microscopic event probabilities for each ion (including: pump absorption, energy transfer/migration, excited states recombination and upconversion emission). The time evolution of the system was divided into a series of events in successive time steps (Δt: 1μs), and each step was accompanied by the possible excited state generation or depletion for every ion following the order of numbers. After each step, the microscopic distribution of excited states was updated to reflect the new energy configuration in the nanoparticle.

1: For each ground state ion, at each time step, we calculated the microscopic probabilities for the pump absorption:

$$P_{abs} = \rho \frac{\sigma \Delta t}{E_{h\upsilon}}$$

where ρ is the excitation power density, σ is the absorption cross section of ion, $E_{h\upsilon}$ is the energy of a single photon and Δt is the time step (*i.e.*1 μs in this work). Then we generate a random number q in the interval [0,1], if q is located into the interval [0, P_{abs}], the ion is excited in this time step, otherwise it keeps to the ground state.

For example, if we assume ρ is 100 W/cm^2, σ is 1.17×10^{-20} cm^2 (referred as the Yb^{3+} ions), and the excitation wavelength is 980 nm, the P_{abs}: the possibility of sensitizer ions being excited within one time step (1 μs) is then calculated as low as 5.76×10^{-6}. Therefore, under the steady state condition, even taking the long lifetime of Yb^{3+} excited state (*i.e.* 1 ms) into account, only dozens of (~ 85) Yb^{3+} ions could be excited simultaneously although the number of Yb^{3+} ions in one single nanoparticle is ~ 1.4×10^4. The very limited number of excited states is beneficial to tracking the time evolution of the system.

2: For each excited ion, we calculated its microscopic probabilities at each time step for the following processes: a) energy transfer, b) energy migration, c) recombination to the ground state without upconversion emission, d) upconversion emission and e) surface quenching (only if the excited states are located on the particle surface). And the probabilities of each event is:

$$P_i = R_i \Delta t$$

where R_i is the rate of each event (as shown in Table S1) and Δt is the time step (*i.e.*1 μs in this work).

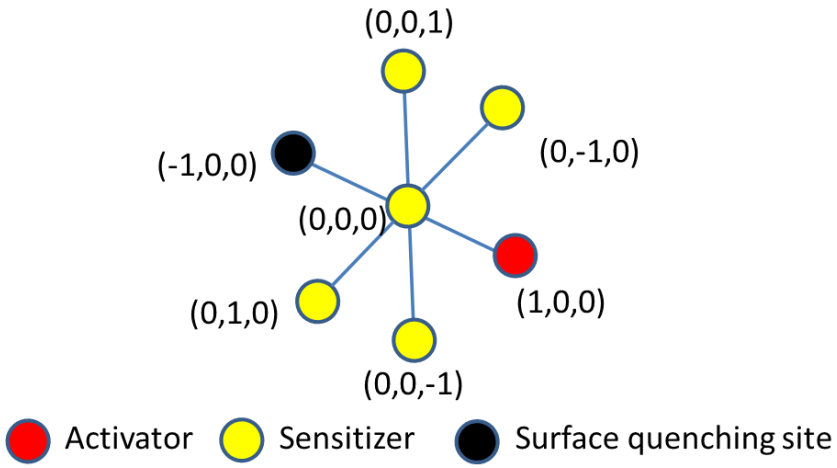

Figure S3. The typical microscopic ions distribution in the sublattice.

Let us turn to the example shown in Figure S3. At step k, if the excitation starts at one sensitizer ion located at the lattice point $A_{x,y,z}$=(0, 0, 0), and we assume that the six nearest neighboring positions around it are 1) one ground state activator ion at the lattice point $A_{1,0,0}$, 2) four ground state sensitizer ions at the lattice point $A_{0,\pm1,\pm1}$ respectively, and 3) one surface quenching site at the lattice point $A_{-1,0,0}$, then the probabilities of each event m_i at step $k+1$ can be obtained as

P_i^k =
- m_1: recombine to the ground state at (0, 0, 0), with 0.001 probability
- m_2: energy transfer to (1, 0, 0), with 0.025 probability
- m_3: energy migration to (0, -1, 0), with 0.1 probability
- m_4: energy migration to (0, 1, 0), with 0.1 probability
- m_5: energy migration to (0, 0, -1), with 0.1 probability
- m_6: energy migration to (0, 0, 1), with 0.1 probability
- m_7: surface quenching to(-1, 0, 0), with 0.1 probability
- m_8: remains the excited state at (0, 0, 0), with 0.474 probability

In the above case, in order to choose which event occurs at step $k+1$, we generate a random number q in the interval [0,1] and choose an event m_i for which

$$q \in [\sum_{i=0}^{m_i-1} P_i^k , \sum_{i=0}^{m_i} P_i^k]$$

recording the time of the event m_i as: $(k+1)\,\Delta t$.

By circularly running the simulation program over 10^6 time steps (*i.e.* over 1 second in the real time), stable statistics output results for one single nanoparticle can be obtained (error less than 15%).

In summary, the algorithm flowchart of steady-state Monte Carlo simulation is shown in Fig. S4.

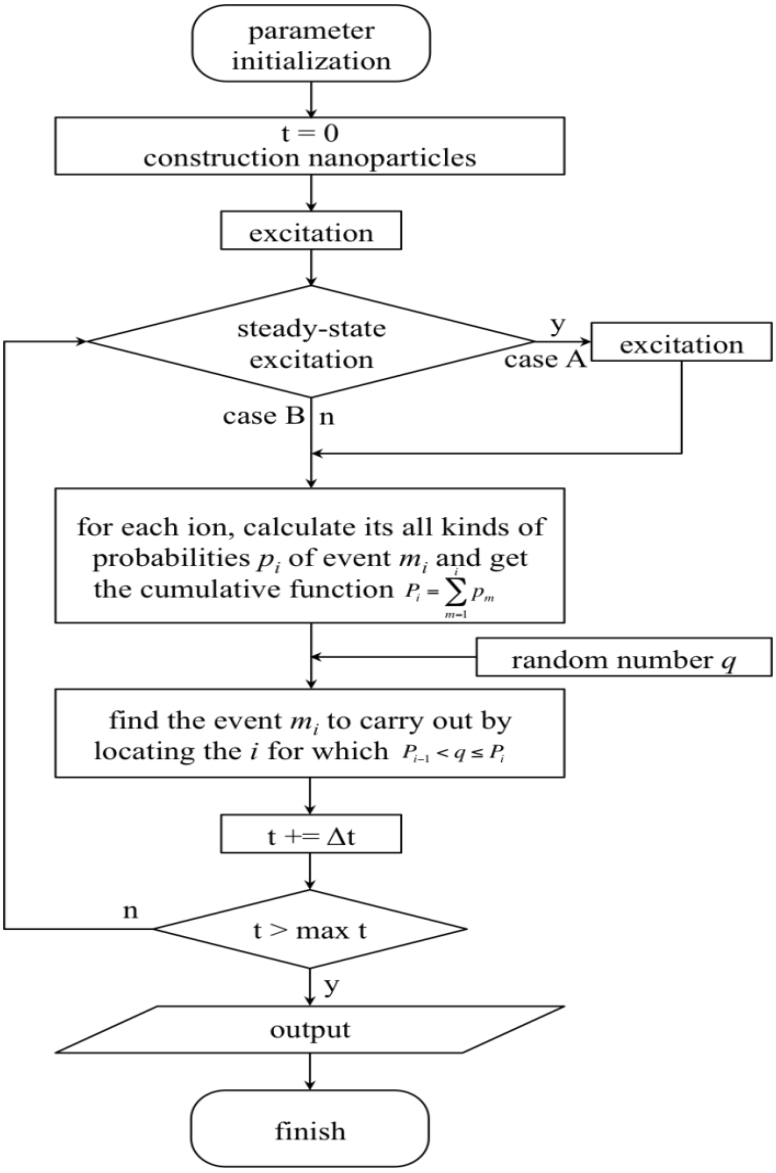

Figure S4. The algorithm flowchart of UC Monte Carlo simulation.

(2) For the time-resolved simulation: for the interaction parameters, compared with the steady-state process, the only difference is the omitted pump absorption process. Typically, we assume 5 ~ 10% sensitizer ions have already been excited at the beginning of the first step, and a long enough time evolution interval (such as 0 ~ 5 ms) is chosen to make sure all the dynamic processes can finish. After that we circulate the running of the simulation program over 10^3 times to obtain the stable statistics output results.

Utilizing the time-resolved simulation, we can understand the $Yb^{3+} \rightarrow Yb^{3+}$ energy migration dynamics from a unique angle:

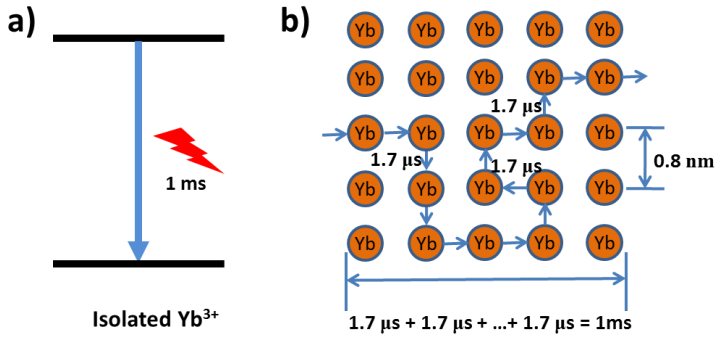

Figure S5. The microscopic manifestation of decay lifetime for a) isolated Yb^{3+}, and b) energy migrated Yb^{3+} in the $NaYF_4$: 20% Yb sublattice.

1) For one isolated Yb^{3+} ion, the lifetime (*e.g.* 1 ms) is the average time of excited state staying at the ion (Fig S5a), which can be calculated by:

$$\tau = \frac{1}{I_0}\int_0^{\infty} I(t)dt$$

where $I(t)$ and I_0 are the luminescence intensity as a function of time t and the maximum emission intensity, respectively.

2) For a sublattice consisting of many Yb^{3+} ions (each ion plays as one grid point), the excited state lifetime will not be affected by the energy migration process. However, its microscopic manifestation has changed: due to the efficient energy migration, the Yb^{3+} excited states tend to migrate among a large number of grid points before relaxing to its ground state, but the time spent on each migrated grid point is correspondingly reduced. For example, we calculate the $Yb^{3+} \rightarrow Yb^{3+}$ energy migration dynamics in an infinite $NaYF_4$: 20% Yb sublattice (Yb^{3+}-Yb^{3+} distance is fixed to 0.8 nm). As shown in the Fig S5b, the expectation value of each step of $Yb^{3+} \rightarrow Yb^{3+}$ energy migration is only ~ 1.7 μs (calculated from the simulation parameters labeled in the Table S1), and the average number of migrated grid point is ~ 600. Therefore, the average "lifetime" of each excited state is still 1 ms. However, if we add Er^{3+} (or energy quenching site) into the sublattice to cut off the energy migration path, obviously, the average "lifetime" of Yb^{3+} excited states will be affected by the number and location of Er^{3+}. Based on this idea, we can efficiently tailor the UC dynamics by controlling the ions distribution in "dopant ions spatial separated" nanostructure.

4: Verification of the simulation

To testify the reasonability of our model, we simulated some macroscopic UC phenomena and compared them with the experimental results.

1): The simulation of UC emission efficiency. As an example, the UC efficiency of the $NaYF_4$: 20% Yb 2%Er@$NaYF_4$ nanostructure (core diameter is 20 nm) was simulated under the excitation power density of 100 W/cm^2 (Table S2).

Table S2: The simulation results for $NaYF_4$: 20% Yb 2%Er@$NaYF_4$ nanostructure (simulation time period: 3 seconds)

Parameters	***Value***	***%***
Absorbed photons	249758	100
Recombined on the S_1 state	195585	78.3
Recombined on the A_1 state	46829	18.7
Recombined on the A_2 state	3627	1.45
UC emission photons	1882	0.75
Excited states number	~ 85	-

As shown in Table S2, the simulated UC efficiency (UC emission photons/Absorbed photons) is 0.75±0.1%, which is in line with the reports.[7] The unique advantage of the Monte Carlo simulation is its relatively clearer microscopic vision. Herein, the simulation results reveal that due to the small absorption cross section of lanthanide ions, only 85 ± 10 excited ions are kept in the overall 15625 grid points under the general excitation density of 100 W/cm^2. Thus the "collision" of the excited states is relatively scarce. In that case, most of the absorbed energy (~ 97%) will be consumed through the sensitizer/activator recombination process (either radiative or nonradiative process) during the random walk period of excited states.

2): The simulation of non-linear relationship between laser power (*P*) and UC intensity (*I*). We simulated the non-linear *p*-*I* relationship ($I=p^n$, n>1), which is also regarded as a feature of UC process. As shown in Fig. S6 (inset), it is easy to find out that in a fixed space, the increased excited states amount will nonlinearly increases the "collision" possibility of excited states. Notably, for a two-photon processes (induced by two excited states "collision"), the simulated *n* value is 1.97 (Fig. S6), which well agrees with the theoretical value (*n*=2).[8]

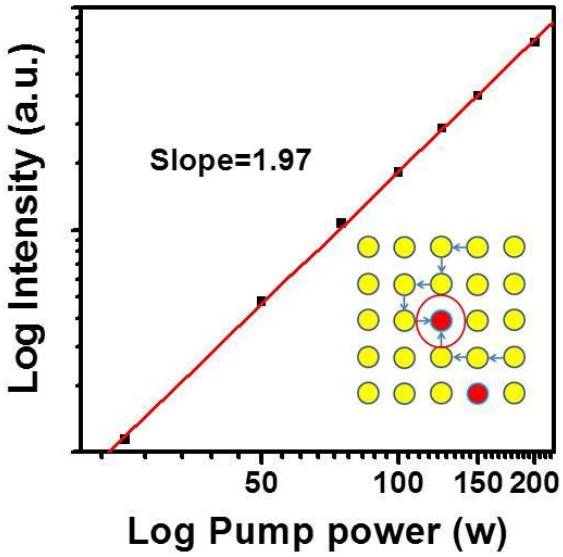

Figure S6. The simulated UC emission intensity as a function of pump power. Inset: the schematic diagram of excited states "collision" induced UC emission.

3): The simulation of surface quenching effect. We also simulated the surface quenching effect of the nanosized UC material. In detail, it is well known that due to the existence of surface defects, organic groups, solvent molecules *etc*, the energy of excited states could be trapped by the surface quenching sites of nanoparticle. Therefore, in our model, we assume that an ion located on the particle surface has a possibility to transfer its energy to the surface quenching sites, and once the energy is trapped by the surface quenching sites, it will be consumed immediately and never come back to the lanthanide ions. So the key point is to determine the surface quenching rate, which could be mutually authenticated by (i) the UC efficiency of bare core nanoparticle and (ii) the experimental and simulation results of particle size dependent UC emission.

(i) Obviously, the UC efficiency of bare core nanoparticle is directly related to the surface quenching rate. As shown in the Table S3, in our model, if the surface quenching rate is set as 10^5 s^{-1}, then for a bare core nanoparticle with a 20 nm diameter, as high as 84.9% excited states will be quenched by the surface quenching sites. Therefore, its UC emission efficiency is significantly decreased to 0.026%, which is well consistent with previous reports.[7]

Table S3: The simulation results for 20 nm $NaYF_4$: 20% Yb 2%Er bare core nanostructure (simulation time period: 3 seconds).

Parameters	***Value***	***%***
Absorbed photons	249758	100
Quenched by surface	211956	84.9
Recombined on the S_1 state	30410	12.2
Recombined on the A_1 state	7107	2.85
Recombined on the A_2 state	135	0.054
UC emission photons	64	0.026
Excited states number	8-15	-

(ii) The other way to verify the surface quenching rate is to analyze the size dependent UC emission of nanoparticle. The smaller the particle size, the stronger the surface quenching effect. As shown in Fig. S7, taking the same surface quenching rate (10^5 s^{-1}) into account, the simulated results of the particle size dependent UC emission intensity do well agree with the experimental results (integration from 500 nm to 700 nm), which confirms the rationality of the surface quenching rate we set up.

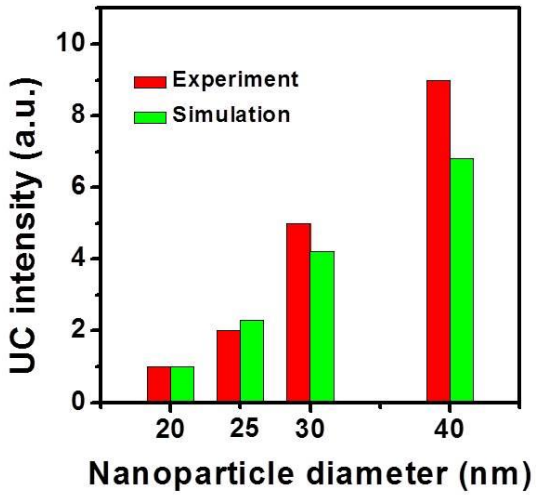

Figure S7. The experimental (red) and simulated (green) results of $NaYF_4$: 20% Yb, 2% Er nanoparticle size dependent UC emission intensity (normalized by the UC intensity of 20 nm bare core nanoparticle).

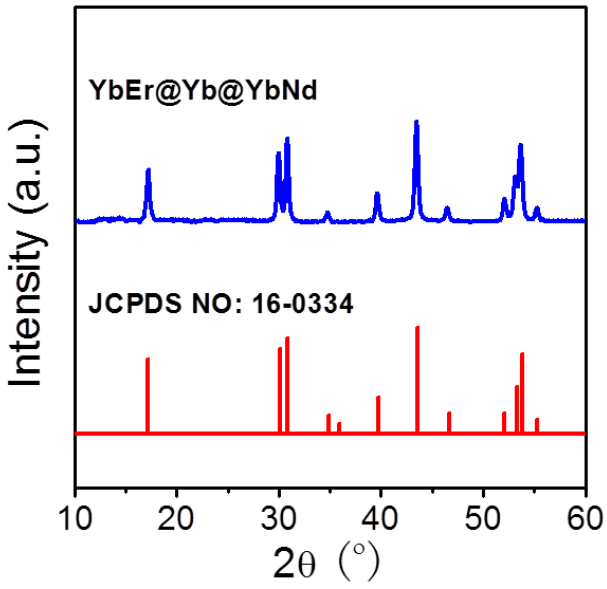

Figure S8. The X-ray powder diffraction of YbEr@Yb@YbNd nanostructure (short for $NaYF_4$: 20% Yb, 2% Er @$NaYF_4$: 20% Yb @$NaYF_4$: 10% Nd, 20%Yb). All the peaks well accord with the standard hexagonal structure of $NaYF_4$ nanoparticles (Joint Committee on Powder Diffraction Standards file number 16-0334).

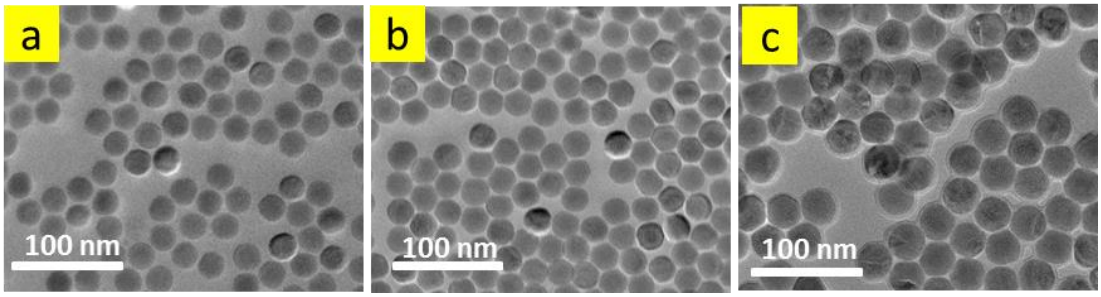

Figure S9. The TEM images of the as-synthesized a) $NaYF_4$: 20% Yb, 2% Er bare core, b) $NaYF_4$: 20% Yb, 2% Er @$NaYF_4$: 20% Yb core-shell and c) $NaYF_4$: 20% Yb, 2% Er @$NaYF_4$: 20% Yb @$NaYF_4$: 10% Nd, 20%Yb core-shell-shell nanostructures. From the TEM images, the size (or thickness) of the core and each shell is measured to be ~ 25.0 nm, ~ 2.8 nm, ~ 3.0 nm.

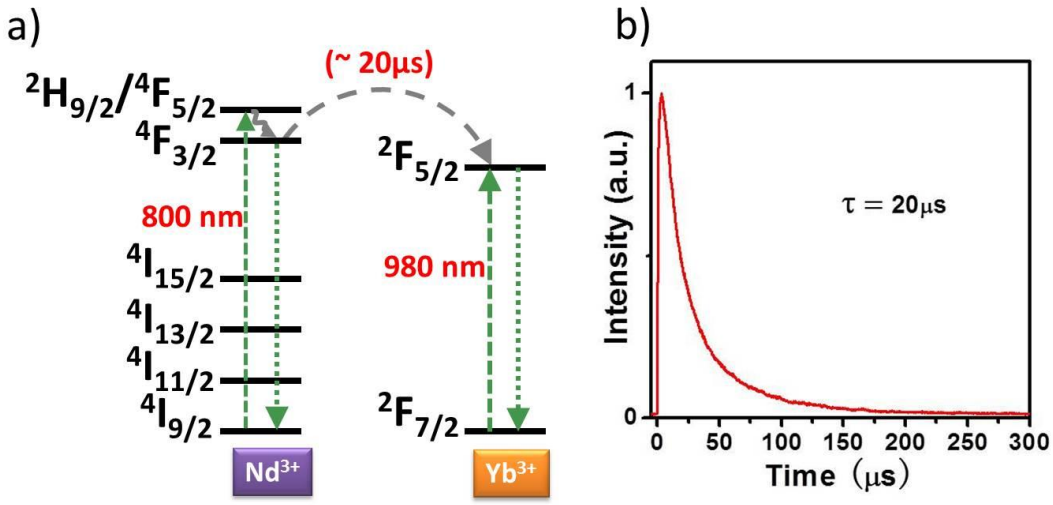

Figure S10. (a) Schematic description of the energy transfer process from Nd^{3+} ($^4F_{3/2}$) to Yb^{3+} ($^2F_{5/2}$), (b)The measured decay lifetime of Nd^{3+} $^4F_{3/2}$ energy state in the $NaYF_4$: 20% Yb, 2% Er @$NaYF_4$: 20% Yb @$NaYF_4$: 10% Nd, 20% Yb nanostructure (excited by 780 nm).

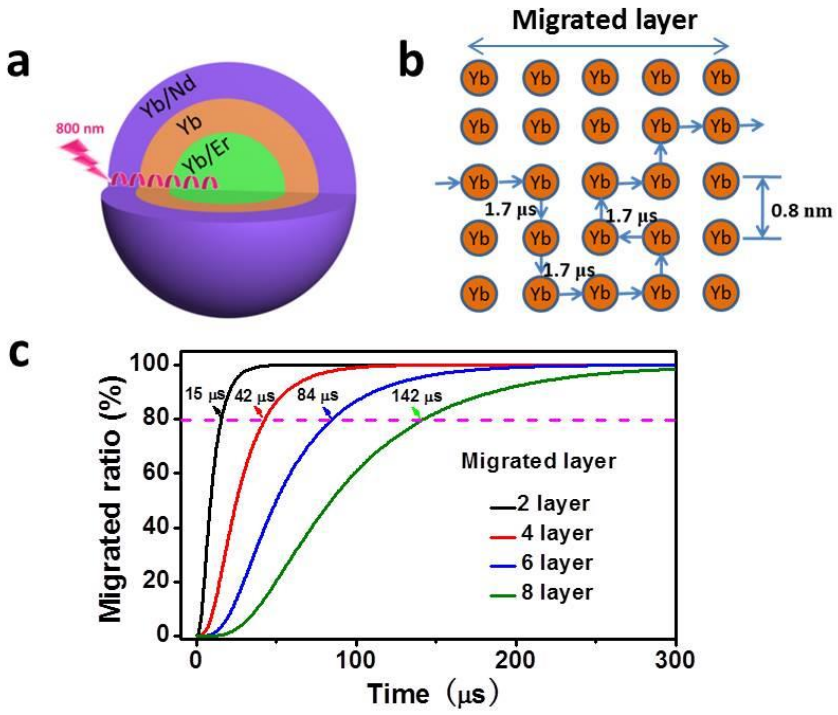

Figure S11. (a) Schematic depiction of energy migration in $NaYF_4$: 20% Yb, 2% Er@$NaYF_4$: 20% Yb@$NaYF_4$: 10% Nd, 20%Yb DISS nanostructure. (b) The energy migration dynamic process among Yb^{3+} ions in the $NaYF_4$: 20% Yb middle layer. (c) The simulated results of the migrated ratio evolution of Yb^{3+} excited states in the middle layers with different thicknesses.

As shown in Fig. S11, for this DISS nanostructure, if targeted by the 80% migrated ratio (we count the time for 80% excited states reaching to the core area at least once), the required migration time is 16 μs, 42 μs, 84 μs and 142 μs for 2, 4, 6, and 8 migrated layer (0.8 nm thickness per layer), respectively (Fig. S11c). It should also be noticed that the Yb^{3+} migration time will be related to but not equal to the corresponding rise or decay modulation time of UC transient emission, since the UC emission is a non-linear process. It relates to a more complicated process – the accumulation and "collision" of excited states. However, our result has already clearly confirmed the non-neglectable energy migration time in the DISS nanostructure.

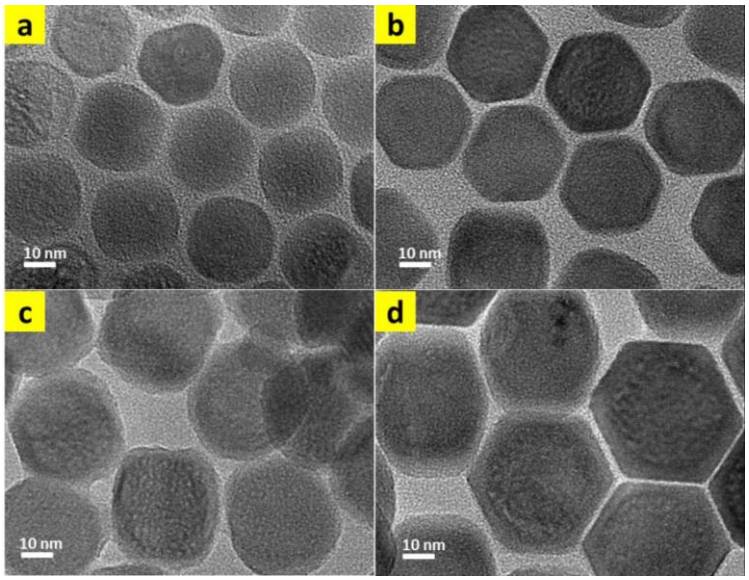

Figure S12. The TEM images of (a) the $NaYF_4$: 20% Yb, 2% Er bare core nanoparticle (~ 25 nm), (b) the $NaYF_4$: 20% Yb, 2% Er @$NaLuF_4$: 20% Nd nanoparticle (~ 30 nm), (c) $NaYF_4$: 20% Yb, 2% Er @$NaLuF_4$: 20% Yb (~ 2.5 nm) @$NaYF_4$: 20% Nd nanoparticle (~ 36 nm), and (d) $NaYF_4$: 20% Yb, 2% Er @$NaLuF_4$: 20% Yb (~ 4.5 nm) @$NaYF_4$: 20% Nd nanoparticle (~ 43 nm). From the contrast of elements Y and Lu in the TEM images, the migration layer ($NaLuF_4$: 20% Yb) thicknesses in b-d are calculated to be 0 nm, ~ 2.5 nm, ~ 4.5 nm, respectively.

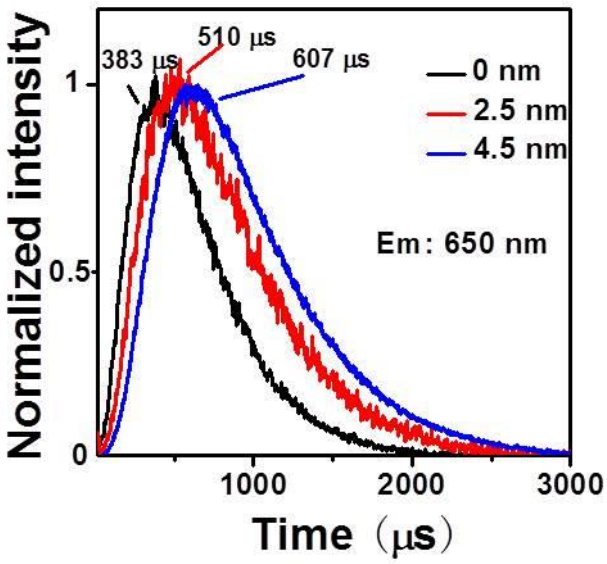

Figure S13. For the $NaYF_4$: 20% Yb, 2% Er @$NaLuF_4$: 20% Yb @$NaYF_4$: 20% Nd series of nanoparticles, the energy migration distance (*i.e.* the middle layer thickness) dependent time-resolved UC luminescence traces monitored at 650 nm. Nanoparticles were excited by 800 nm. The numbers in the picture are the corresponding middle layer ($NaLuF_4$: 20% Yb) thicknesses.

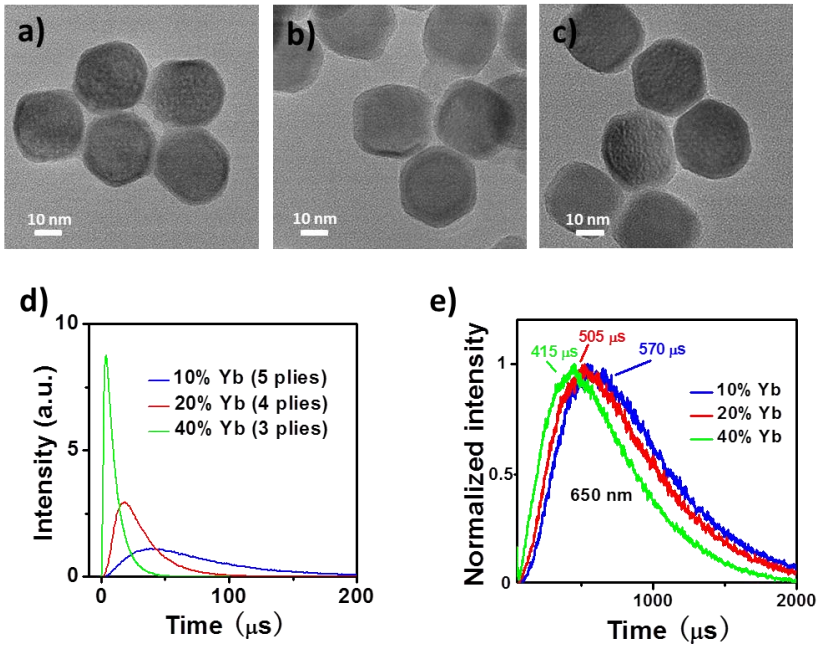

Figure S14. The TEM images of the YbEr@x%Yb@Nd nanostructure (middle layer thickness is fixed to ~ 2.5 nm) with different Yb^{3+} dopant concentrations in the middle layers (a) x=10, (b) x=20, (c) x=40. For the 800 nm excited YbEr@x%Yb@Nd nanostructure: (d) the distribution of simulated migration time to go through the 3 nm thick middle layer, (e) the experimental results of time-resolved 650 nm UC luminescence traces with ~ 2.5 nm thick middle layer.

Table S4: The calculated parameters for the $NaYF_4$: 20% Yb, 2% Er (25 nm) @$NaLuF_4$: x% Yb (3 nm) @$NaYF_4$: 20% Nd (x=10, 20, 40) nanostructures.

Yb^{3+} doping concentration	$Yb^{3+} \rightarrow Yb^{3+}$ energy migration rate	Yb^{3+}-Yb^{3+} distance	Yb^{3+}-Yb^{3+} plies
10%	2×10^4 s^{-1}	1.0 nm	3
20%	1×10^5 s^{-1}	0.8 nm	4
40%	1×10^6 s^{-1}	0.63 nm	5

As shown in Fig S14 and Table S4, for the 800 nm excited YbEr@x%Yb@Nd nanostructure, increasing Yb^{3+} dopant concentration in the middle layer results in two opposite effects. Firstly, it speeds up the $Yb^{3+} \rightarrow Yb^{3+}$ energy migration rate, as mentioned above, the doping concentration related migration rates could be obtained from the quantum mechanics calculations (we also give an example in the above).[6] Secondly, it decreases the Yb^{3+}-Yb^{3+} distance, leading to increasing the number of Yb^{3+}-Yb^{3+} plies in a fixed distance (*e.g.* 3 nm in Table S4). The simulation (Fig. S14d, the middle layer is fixed to 3 nm) and experimental results (Fig. 3d and Fig. S14e, the middle layer is measured to ~ 2.5 nm) all indicated that: with the Yb^{3+} dopant concentration increasing (from 10% to 40%), the effect of rapid increased energy migration rate (from 2×10^4 s^{-1} to 1×10^6 s^{-1}) will cover the effect of increased Yb^{3+}-Yb^{3+} plies (from 3 to 5), thus leading to a shortened rise edge.

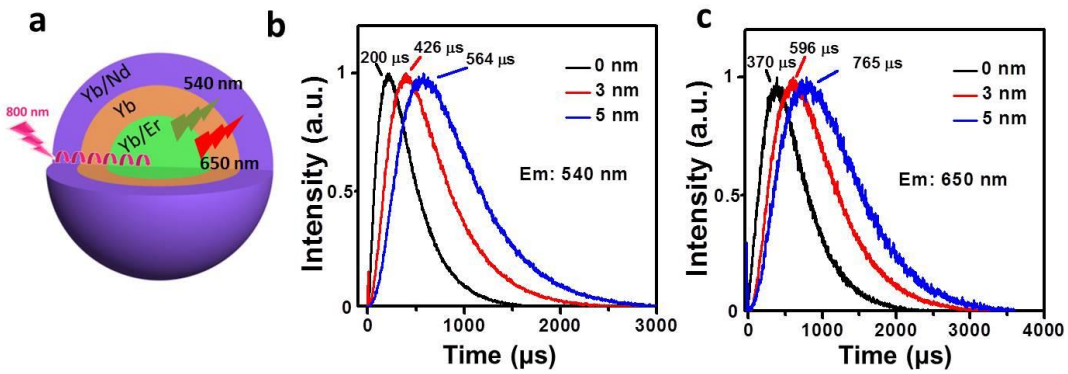

Figure S15. (a) Schematic depiction of the UC process in the $NaYF_4$: 20% Yb, 2% Er @$NaYF_4$: 20% Yb @$NaYF_4$: 10% Nd, 20%Yb core/shell/shell DISS nanostructure under 800 nm excitation. (b) The 540 nm time-resolved UC luminescence traces and (c) the 650 nm time-resolved UC luminescence traces by varying the middle layer thickness (excited by 800 nm, the numbers in the pictures are the corresponding middle layer thicknesses).

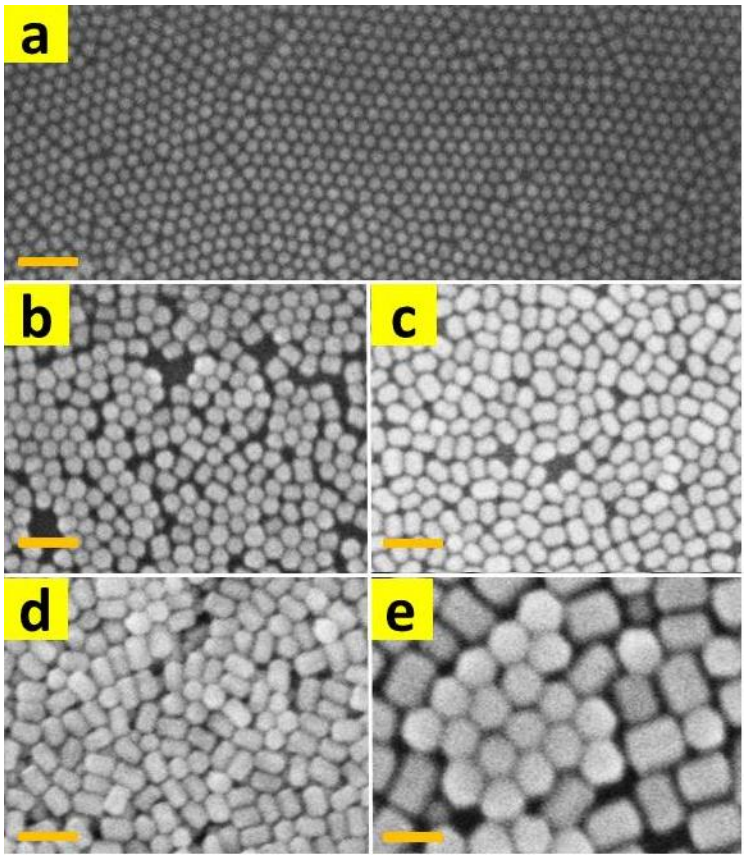

Figure S16. The SEM images of the $NaYF_4$: 20% Yb, 2% Er (20 nm) @$NaYF_4$: 20% Yb core/active shell series of nanoparticles with different active shell thicknesses: (a) 0 nm (bare core), (b) 3 nm, (c) 6 nm, (d) 10 nm and (e) 15 nm. The scale bars in the pictures are all 50 nm.

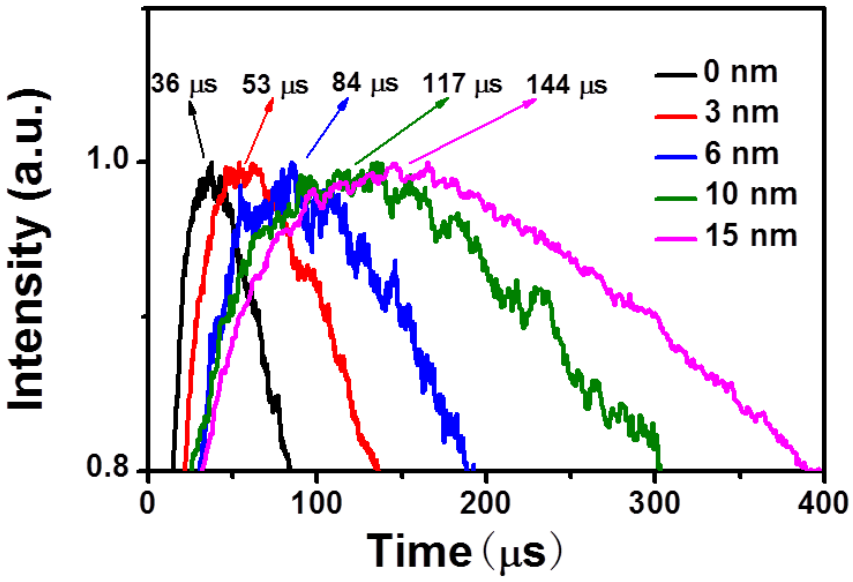

Figure S17. Rise edge of the shell thickness dependent 540 nm UC emission from the $NaYF_4$: 20% Yb, 2% Er (20 nm) @$NaYF_4$: 20% Yb core/active shell series of DISS nanoparticles. Nanoparticles are excited at 980 nm. The shell thicknesses and corresponding consuming times of rise edges are indicated in the Figure.

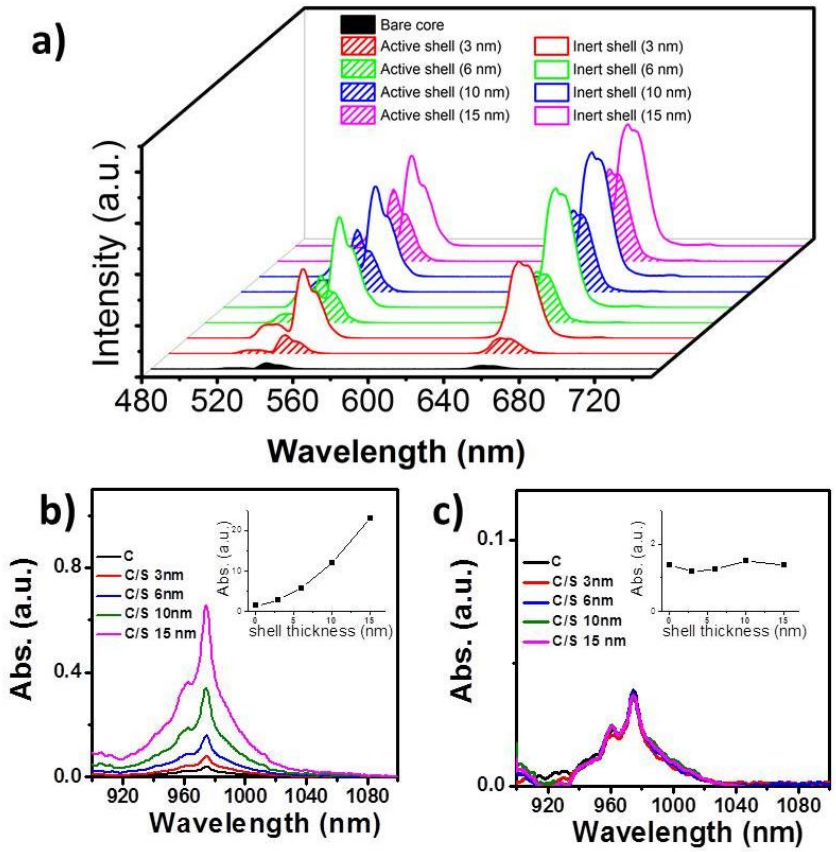

Figure S18. (a) The UC emission spectra of series of $NaYF_4$: 20% Yb, 2% Er@$NaYF_4$: 20% Yb core/active shell structures and $NaYF_4$: 20% Yb, 2% Er@$NaYF_4$ core/inert shell structures. (b) Absorption spectra of the series of core/active shell structures. Insert: the integral area of the absorption peak (from 920 nm to 1040 nm). (c) Absorption spectra of the series of core/inert shell structures. Insert: the integral area of the absorption peak (from 920 nm to 1040 nm).

As shown in Figure S18a, despite that the UC emission intensity of core/active shell structures keeps enhancing with the shell thickness increasing, the intensity of either ~ 540 nm or ~ 650 nm emission is always lower than the corresponding core/inert shell structures (the one with the same shell thickness). Especially when we consider the additional absorption increase because of the active shell (Fig. S18b), the UC efficiency (calculated by: emission intensity/absorption intensity) of core/active shell structures is obviously much lower than the corresponding core/inert shell structures.

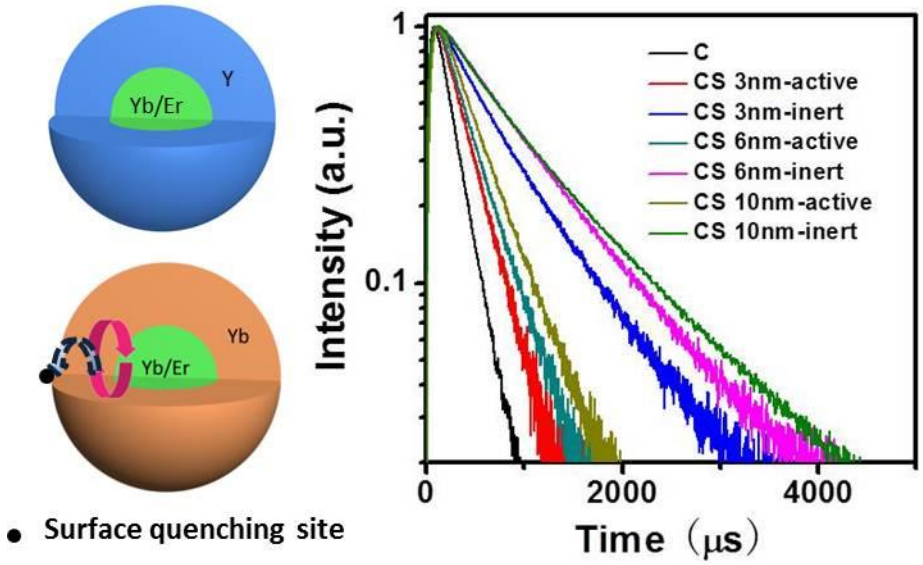

Figure S19. The decay lifetime traces of Yb^{3+} ($^2F_{5/2}$ excited state) in core/inert shell ($NaYF_4$: Yb, Er@$NaYF_4$) and core/active shell ($NaYF_4$: Yb, Er@$NaYF_4$: 20% Yb) nanostructures. The excitation wavelength is 980 nm and the emission is at 1040 nm.

Table S5: The Yb^{3+} ($^2F_{5/2}$ excited state) decay lifetimes in core/inert shell and core/active shell nanostructures.

Sample	Decay lifetime	
	Active (μs)	Inert (μs)
bare core	205	205
3nm shell	307	648
6 nm shell	345	804
10 nm shell	392	857

As shown in Fig.S19 and Table S5, the Yb^{3+} $^2F_{5/2}$ excited state decay lifetimes are significantly shortened in the core/active shell structures (compared with the corresponding core/inert shell structures). The results indicate the efficient energy back transfer (energy migrates from core to active shell and is finally quenched by surface quenching sites) is occurred in the core/active shell structure, subsequently decreasing the UC intensity of the core/active shell nanoparticles.

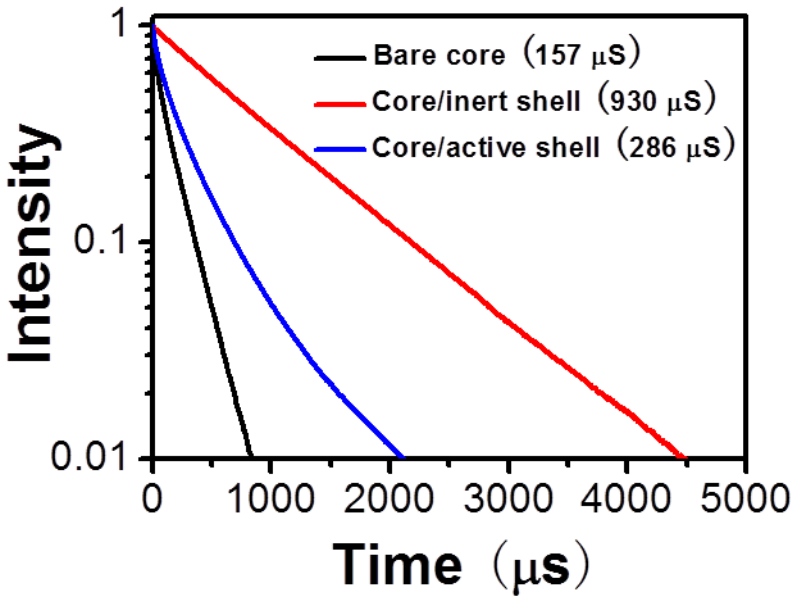

Figure S20. The simulation results of Yb^{3+} ($^2F_{5/2}$ energy state) decay lifetimes of $NaYF_4$: 20% Yb, 2% Er bare core (black curve), YbEr@Y core/inert shell (red curve) and YbEr@Yb core/active shell (blue curve) nanoparticles. The shell thickness is fixed at 6 nm.

Table S6: The simulation results for core/inert shell and core/active shell nanoparticles (shell thickness : 6 nm, simulation time period: 3 seconds).

Parameters	*Inert shell*	*Active shell*
Absorbed photons	249758	1006378
Quenched by surface	0	764338
UC emission photons	1882	446
UC efficiency	0.75%	0.044%

According to the simulation results listed in Figure S20 and Table S6, on the condition of 6 nm shell thickness, due to the harmful energy back transfer effect (from core to active shell), ~ 76% Yb^{3+} excited states are quenched by the surface quenching sites in the $NaYF_4$: Yb, Er@$NaYF_4$: 20% Yb core/active shell nanostructure. Therefore, compared with the $NaYF_4$: Yb, Er@$NaYF_4$ core/inert shell structure, despite the core/active shell structure owns the higher absorption ability (about 3 times higher than core/inert shell structure), 1) its Yb^{3+} ($^2F_{5/2}$ excited state) decay lifetime is much shorter and 2) its UC intensity is much weaker, which is well in line with the experimental results.

References

[1] H. S. Qian, Y. Zhang, *Langmuir* **2008**, *24*, 12123-12125.

[2] N. J. J. Johnson, A. Korinek, C. Dong, F. C. J. M. van Veggel, *J. Am. Chem. Soc.* **2012**, *134*, 11068-11071.

[3] a) S. Fischer, N. D. Bronstein, J. K. Swabeck, E. M. Chan, A. P. Alivisatos, *Nano Lett.* **2016**, *16*, 7241-7247; b) R. Deng, J. Wang, R. Chen, W. Huang, X. Liu, *J. Am. Chem. Soc.* **2016**, *138*, 15972-15979; c) Y. Zhong, I. Rostami, Z. Wang, H. Dai, Z. Hu, *Adv. Mater.* **2015**, *27*, 6418-6422; d) M. Y. Hossan, A. Hor, Q. Luu, S. J. Smith, P. S. May, M. T. Berry, *J. Phys. Chem. C* **2017**, *121*, 16592-16606.

[4] a) Y. F. Wang, G. Y. Liu, L. D. Sun, J. W. Xiao, J. C. Zhou, C. H. Yan, *ACS Nano* **2013**, *7*, 7200-7206; b) L. Tu, X. Liu, F. Wu, H. Zhang, *Chem. Soc. Rev.* **2015**, *44*, 1331-1345.

[5] F. Auzel, *Chem. Rev.* **2004**, *104*, 139-173.

[6] T. Kushida, *J. Phys. Soc. Jpn.* **1973**, *34*, 1318-1326.

[7] J. C. Boyer, F. C. J. M. van Veggel, *Nanoscale* **2010**, *2*, 1417-1419.

[8] M. Pollnau, D. R. Gamelin, S. R. Luthi, H. U. Gudel, M. P. Hehlen, *Phys. Rev. B* **2000**, *61*, 3337-3346.